Netsu Sokutei **25** (5) 141-149

論 文

Phase Transition of Monoclinic Hydroxyapatite

Toshiyuki Ikoma*, Atsushi Yamazaki*, Satoshi Nakamura** and Masaru Akao**

(Received November 2, 1998; Accepted November 26, 1998)

Monoclinic hydroxyapatite was prepared by a wet method and followed by heating in air at 1473 K for 1 hour, and its phase transition was investigated by a high temperature X-ray powder diffractometry and a differential scanning calorimetry. The prepared hydroxyapatite was 98 % monoclinic. The Rietveld refinement results revealed that the low temperature phase had monoclinic symmetry, space group $P2_1/b$ and the high temperature phase had hexagonal symmetry, space group $P6_3/m$. In monoclinic hydroxyapatite, two different sizes of oxygen triangles existed. The rotation of phosphate tetrahedra at about 6° and the change of the hydroxyl order to disorder arrangement occurred due to the phase transition. The phase transition took place reversibly at 480.5(1) K in heating process and 477.5(1) K in cooling process. The enthalpy value was found to be 130(1) J mol^{-1}. Further, the transition was observed to resolve into two steps that were attributed to the rotation of phosphate tetrahedra and the order to disorder arrangement of hydroxyls.

1. Introduction

Hydroxyapatite ($Ca_5(PO_4)_3OH$) has been widely investigated for the chemical and physical properties (*e.g.* crystal structure,[1-3] dissolution property[4-6] and surface structure),[7-9] because it is a main inorganic component of vertebrate bone and tooth tissues. Hydroxyapatite is classified as a bioactive material, which bonds to hard tissues directly. Hydroxyapatite has been thought to be isostructural with flourapatite ($Ca_5(PO_4)_3F$) and has hexagonal symmetry with the space group $P6_3/m$.[2, 10] Elliott *et al.*[3] firstly reported the crystal structure of a monoclinic hydroxyapatite single crystal (space group of $P2_1/b$) that was prepared by heating a chlorapatite single crystal in steam at 1473 K for 2 weeks.[11] The sample was mimetically twined and was 37 % monoclinic. The chlorapatite ($Ca_5(PO_4)_3Cl$) has also monoclinic symmetry, space group $P2_1/b$.[12] The monoclinic hydroxyapatite has pseudohexagonal symmetry and the doubled *b*-axis lattice parameter compared with the hexagonal unit cell. The structure of hydroxyapatite has been thought to be sensitive to its chemical composition and to be changed by preparation methods. Monoclinic hydroxyapatites have been synthesized by both dry methods[13] and hydrothermal methods,[14] but not yet by wet methods.[15]

Van Ree *et al.*[14] synthesized hydroxyapatite and deuterohydroxyapatite single crystals by the hydrothermal method and reported the monoclinic to hexagonal phase transition at 484.5 K under a polarized light microscope equipped with hot stage. They described that the phase transition was a simple order-disorder phase transition. Suda *et al.*[13] also reported the phase transition of hydroxyapatite (Ca/P ratio; 1.68), which was

* Department of Resources and Environmental Engineering, School of Science and Engineering, Waseda University, 3-4-1 Okubo, Shinjuku-ku, Tokyo 169-8555, Japan

**Institute for Medical and Dental Engineering, Tokyo Medical and Dental University, 2-3-10 Surugadai, Kanda, Chiyoda-ku, Tokyo 101-0062, Japan

prepared by the dry method, using a differential scanning calorimetry and a high temperature X-ray powder diffraction method. The phase transition occurred reversibly at 480.3 K in heating process and at 479.7 K in cooling process.

Hydroxyapatite has been thought to be an ion conductive material.[16), 17)] The ion conductivity was mainly caused by the hydroxyl ions mobility at high temperature (up to about 873 K). As described above, the hydroxyl ion's behavior for the dependence on temperatures has been very important. However, the crystal structure details of monoclinic hydroxyapatite at high temperatures and the details of its phase transition have not been fully understood.

In the present paper, the phase transition mechanism was described. The monoclinic hydroxyapatite was prepared by a wet method and followed by heating in air at 1473 K for 1 hour. The temperature and enthalpy of the phase transition were measured by a differential scanning calorimetry. The thermal expansion and phase transition mechanism were discussed from the Rietveld refinements using the high temperature X-ray powder diffraction data at 300, 473 and 673 K.

2. Experimental Procedure

2.1 Synthesis and Chemical Composition

The details of preparation method were already reported.[18)] The monoclinic hydroxyapatite was prepared as followed. 4000 ml of a 0.6 mol l^{-1} H_3PO_4 solution were added in drops slowly into 8000ml of a vigorously stirred 0.5 mol l^{-1} $Ca(OH)_2$ suspension to the final pH of 7.5 at the room temperature. The resulting hydroxyapatite suspension was filtered and dried at 333 K for 24 hours and heated in air at 1473 K for 1 hour. The sample was slowly cooled to the room temperature.

The calcium and phosphorus contents were determined by an inductively coupled plasma emission spectrometry. The chemical formula was determined as $Ca_{4.95}(PO_4)_{2.99}(OH)_{0.92}$; the hydroxyl content was calculated from the charge neutrality of calcium and phosphate ion contents. The Ca/P ratio was 1.65 and calcium and hydroxyl ions were slightly deficient.

2.2 Structural Analysis

X-ray powder diffraction measurements for the prepared hydroxyapatite were conducted at 300, 473 and 673 K on a Rigaku Rint-2500 diffractometer with graphite monochromatized Cu$K\alpha$ radiation at 50 kV and 300 mA using a platinum sample holder. The temperature was raised at the heating rate of 2 K min^{-1} and held for 1 hour at the objective temperatures. Then, the intensity data were collected twice in 0.02° steps with the counting time of 6.5 seconds, in the 2θ range of 20° to 110°. The divergence, scatter and receiving slits were 1/2°, 1/2° and 0.15 mm, respectively. Averaged intensity data of the twice measurements were adopted for Rietveld refinements.

The crystal structures of the hydroxyapatites at each temperature were refined by the program, RIETAN-97.[19)] Two phases of hydroxyapatite and platinum were confirmed from the diffraction patterns. The Rietveld refinements were performed at two phases. The structural refinements of the hydroxyapatites at 300 K and 473 K were performed based on monoclinic symmetry, space group $P2_1/b$ (No.14). The monoclinic cell setting has the c-axis as the unique axis. The initial atomic coordinates and the lattice parameters of monoclinic hydroxyapatite were used from the reported data.[18)] The crystal structure of hydroxyapatite at 673 K was refined based on hexagonal symmetry, space group $P6_3/m$ (No.176). The atomic coordinates reported by Kay *et al.*[2)] were used as the initial parameters of hexagonal hydroxyapatite. Refining the structures at 300 K and 473 K, the individual isotropic thermal parameters were determined to be nonpositive, and these were constrained to be equal for the same atoms. Refining the structure at 673 K, the thermal parameters were refined as anisotropic thermal parameters. The β_{22} and β_{12} of Ca(1) and O(H) sites are restrained to be $\beta_{22} = \beta_{11}$ and $\beta_{12} = \beta_{11} / 2$ from the symmetry operations. All the structures were determined without hydrogen atoms and the occupancy factors exclusive of hydroxyl oxygen (O(H)) in the hexagonal hydroxyapatite were assumed to be 1.0. The occupancy factor of hydroxyl oxygen (O(H)) in the hexagonal hydroxyapatite at 673 K was assumed to be 0.5.

The monoclinic percentages were calculated, assuming to be three phases of monoclinic, hexagonal hydroxyapatite and platinum using the intensity data collected at 300 K. The scale parameters were only refined.

2.3 Differential Scanning Calorimetry

The temperature and enthalpy of the phase transi-

tion were analyzed with a differential scanning calorimeter (Perkin-Elmar Pyris 1). The sample weight was 31.07 mg and the sample was crimped in an aluminum sample holder. The analyses were carried out under an argon gas flow condition in the temperature range of 393 K to 573 K, and at the heating and / or cooling rate of 20, 10, 5 and 2 K min^{-1}. Before the measurements were started, the temperature was held at 393 K for 15 minutes. These measurements were iterated three times. The temperature was calibrated by measuring the melting point of indium (In) at 429.60 K.

3. Results and Discussion

3.1 Structure Changes at Each Temperature

Monoclinic hydroxyapatite has the doubled *b*-axis parameter compared with hexagonal hydroxyapatite, the unit cell content (*Z*) is 4. The origin of a monoclinic cell was shifted toward (0, −1/2, 0) in the hexagonal unit cell. The monoclinic unit cell has a two-fold screw axis on the *c*-axis and *b*-glide planes perpendicular to the two-fold axis. In hexagonal hydroxyapatite, the *b*-glide planes are changed to mirror planes and the unit cell content (*Z*) is 2. The monoclinic percentage of the prepared hydroxyapatite was calculated to be 98 %. The sample, therefore, was a single phase of monoclinic symmetry. **Table 1** shows the results of the Rietveld refinements at 300, 473 and 673 K, respectively. **Fig.1**, **Fig.2**, and **Fig.3** depict the Rietveld refinement's plots at 300, 473 and 673 K in the 2θ range of 20° to 110°. No other phases of calcium phosphates were observed

Table 1 Details of Rietveld refinements for hydroxyapatite.

	Measured Temp./K		
	300	473	673
R_{wp} / %	6.11	5.85	6.01
R_P / %	4.43	4.33	4.43
R_e / %	4.72	4.70	4.64
Hydroxyapatite			
Crystal system	monoclinic	monoclinic	hexagonal
Space group	$P2_1/b$ (No.14)	$P2_1/b$	$P6_3/m$ (No.176)
Z	4	4	2
D_x / g cm^{-3}	3.14	3.13	3.11
Cell parameters	a = 0.9427(2)	a = 0.9442(2)	a = 0.9465(2)
/ nm or °	b = 1.8856(4)	b = 1.8884(4)	
	c = 0.6888(1)	c = 0.6896(1)	c = 0.6910(1)
	γ = 119.98(1)	γ = 120.00(1)	
Weight percent	99.3	99.2	99.5
/ %			
Platinum			
Space group	$Fm3m$ (No.225)	$Fm3m$	$Fm3m$
Cell parameters	0.39258(6)	0.39309(6)	0.39359(6)
/ nm			
Weight percent			
/ %	0.7	0.8	0.5

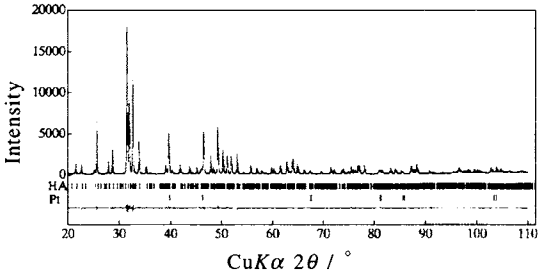

Fig.1 Rietveld refinement plots of hydroxyapatite at 300 K.

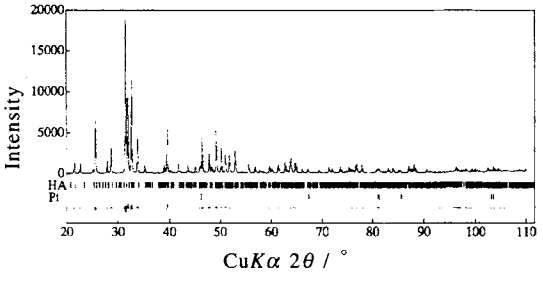

Fig.2 Rietveld refinement plots of hydroxyapatite at 473 K.

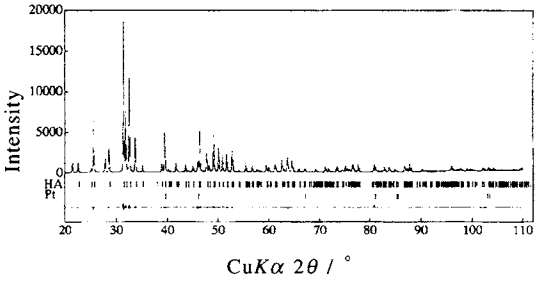

Fig.3 Rietveld refinement plots of hydroxyapatite at 673 K.

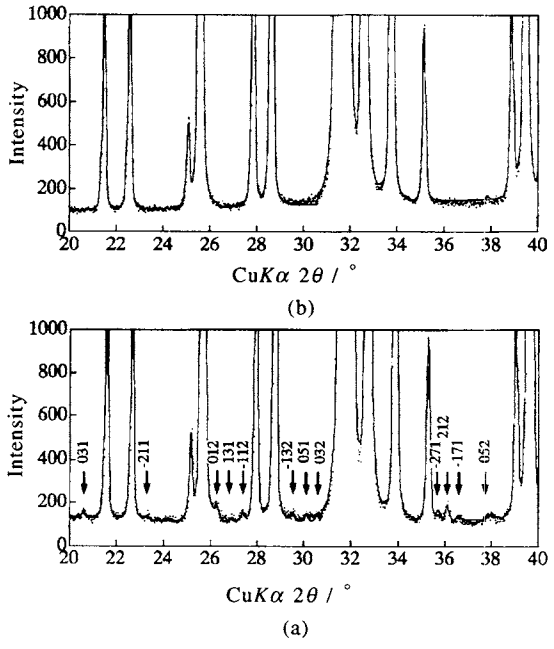

Fig.4 Observed and calculated patterns of hydroxyapatite at 300 K (a) and 673 K (b). The arrows represent the characteristic reflections of monoclinic hydroxyapatite.

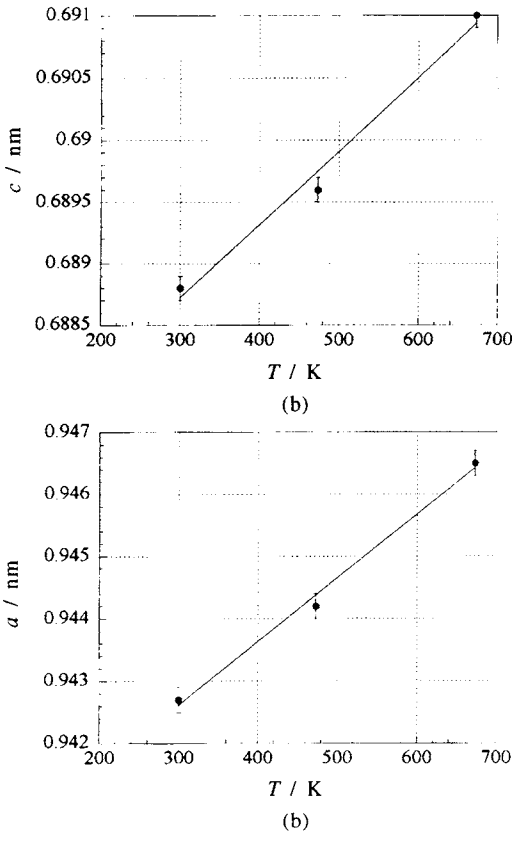

Fig.5 The changes of *a*-axis lattice parameters (a) and *c*-axis parameters (b) at 300 K, 473 K and 673 K.

except for platinum. The hydroxyapatites at 300 K and 473 K had monoclinic symmetry, space group $P2_1/b$. However, the hydroxyapatite at 673 K had hexagonal symmetry, space group $P6_3/m$. The observed and calculated X-ray powder diffraction patterns in the 2θ range of 20° to 40° are shown in **Fig.4**(a) at 300 K and **Fig. 4**(b) at 673 K. The arrows in **Fig.4**(a) represent characteristic reflections of monoclinic hydroxyapatite. The Miller indices and 2θ angles of the characteristic reflections were matched to the reported values.[20] These reflections were very weak, but were detectable in the measurements. The characteristic reflections disappeared completely in **Fig.4**(b). This means that the structure of hydroxyapatite at 673 K was changed from the monoclinic to hexagonal symmetry.

Table 1 also shows the lattice parameters of hydroxyapatites and platinums at 300, 473 and 673 K, respectively. The lattice parameters of the monoclinic hydroxyapatite at 300 K were the almost same as the reported ones.[3] **Fig.5** shows the *a*-axis and the *c*-axis parameter's changes against the temperatures. The *a*-axis and the *c*-axis parameters were linearly varied with the temperatures. The mean thermal lattice expansion coefficients of the hydroxyapatite in the region from 300 K to 673 K were calculated to be $\alpha_a = 10.8 \times 10^{-6}$ K^{-1} and $\alpha_c = 8.56 \times 10^{-6}$ K^{-1}, and $\alpha = 6.90 \times 10^{-6}$ K^{-1} for the platinum.

Table 2, 3 and **4** show the refined atomic parameters of the hydroxyapatites at 300, 473 and 673 K, respectively. The atomic parameters of monoclinic hydroxyapatites were similar to the reported ones[3] without that of the hydroxyl oxygen. Ca(1) and Ca(2) sites in monoclinic hydroxyapatite are crystallographically equivalent to Ca(1) site in hexagonal hydroxyapatite and Ca(3), Ca(4) and Ca(5) site are to Ca(2) site. Moreover, O(1), O(4), O(7) and O(10) sites in monoclinic hydroxyapatite are crystallographically equivalent to O(1) site in hexagonal hydroxyapatite and O(2), O(5), O(8) and O(11) sites are to O(2) site and the other oxygen

Table 2 Structural parameters of hydroxyapatite measured at 300 K.

atom	site	x	y	z	B / Å^2
Ca^{2+}(1)	4*e*	0.3390(21)	0.5833(8)	0.0022(6)	0.32(2)
Ca^{2+}(2)	4*e*	0.3204(19)	0.5782(8)	0.4998(6)	0.32
Ca^{2+}(3)	4*e*	0.2507(18)	0.2481(11)	0.2468(12)	0.32
Ca^{2+}(4)	4*e*	-0.0063(22)	0.6244(10)	0.7562(15)	0.32
Ca^{2+}(5)	4*e*	0.2560(21)	0.3734(12)	0.7442(15)	0.32
P(1)	4*e*	0.398(3)	0.433(1)	0.249(2)	0.34(4)
P(2)	4*e*	0.629(3)	0.262(1)	0.249(2)	0.34
P(3)	4*e*	0.034(3)	0.451(1)	0.750(2)	0.34
O (1)	4*e*	0.322(7)	0.491(3)	0.243(3)	0.39(5)
O (2)	4*e*	0.477(5)	0.329(3)	0.735(3)	0.39
O (3)	4*e*	0.150(4)	0.579(2)	0.256(4)	0.39
O (4)	4*e*	0.589(4)	0.484(2)	0.262(3)	0.39
O (5)	4*e*	0.533(6)	0.310(3)	0.260(3)	0.39
O (6)	4*e*	0.126(5)	0.544(3)	0.761(3)	0.39
O (7)	4*e*	0.357(4)	0.383(2)	0.067(5)	0.39
O (8)	4*e*	0.747(4)	0.291(2)	0.068(5)	0.39
O (9)	4*e*	0.087(4)	0.432(2)	0.544(4)	0.39
O (10)	4*e*	0.344(4)	0.378(2)	0.425(6)	0.39
O (11)	4*e*	0.749(4)	0.292(2)	0.427(6)	0.39
O (12)	4*e*	0.074(4)	0.410(2)	0.915(5)	0.39
O (H)	4*e*	0.004(5)	0.249(4)	0.196(1)	1.0(3)

sites are to O(3) site. **Fig.6** and **Fig.7** depict the structure of the hydroxyapatites refined at 300 K and 673 K with ellipsoids plotted at the 50 % probability level, and the arrangements of the calcium and oxygen triangles around the hydroxyl column are illustrated. The monoclinic hydroxyapatite (**Fig.6**) has two equivalent calcium triangles formed by Ca(3), Ca(4) and Ca(5) normal to a hydroxyl column at about $z = 1/4$, 3/4 and four oxygen triangles that constitute phosphate tetrahedra formed by O(7), O(8) and (9) and O(10), O(11) and O(12) normal to the hydroxyl column. In the four oxygen triangles, two independent oxygen triangles exist at the upper and lower sides against the calcium triangles at about $z = 1/4$, 3/4 in its unit cell. In hexagonal hydroxyapatite (**Fig.7**), there are two equivalent regular calcium triangles formed by Ca(2) lied on the mirror planes at $z = 1/4$, 3/4 and four equivalent regular oxygen triangles formed by O(3), which triangles are located perpendicular to the six-fold screw axis (the *c*-axis).

Table 5 shows the interatomic distances around a

Table 3 Structural parameters of hydroxyapatite measured at 473 K.

atom	x	y	z	B / Å^2
Ca^{2+}(1)	4*e* 0.3380(18)	0.5838(11)	0.0012(6)	0.60(2)
Ca^{2+}(2)	4*e* 0.3208(17)	0.5830(11)	0.4990(7)	0.60
Ca^{2+}(3)	4*e* 0.2478(29)	0.2489(9)	0.2476(11)	0.60
Ca^{2+}(4)	4*e* -0.0092(26)	0.6227(14)	0.7552(16)	0.60
Ca^{2+}(5)	4*e* 0.2570(23)	0.3749(10)	0.7465(16)	0.60
P(1)	4*e* 0.398(3)	0.434(2)	0.248(2)	0.54(5)
P(2)	4*e* 0.634(3)	0.264(1)	0.250(2)	0.54
P(3)	4*e* 0.034(2)	0.453(1)	0.747(2)	0.54
O (1)	4*e* 0.321(4)	0.487(2)	0.249(3)	0.77(6)
O (2)	4*e* 0.486(5)	0.329(3)	0.741(3)	0.77
O (3)	4*e* 0.153(6)	0.583(2)	0.238(4)	0.77
O (4)	4*e* 0.585(6)	0.483(3)	0.259(4)	0.77
O (5)	4*e* 0.548(3)	0.313(2)	0.247(3)	0.77
O (6)	4*e* 0.121(5)	0.546(3)	0.766(3)	0.77
O (7)	4*e* 0.356(5)	0.380(2)	0.064(5)	0.77
O (8)	4*e* 0.745(3)	0.286(1)	0.062(4)	0.77
O (9)	4*e* 0.091(4)	0.436(2)	0.548(4)	0.77
O (10)	4*e* 0.343(4)	0.376(2)	0.424(5)	0.77
O (11)	4*e* 0.753(3)	0.289(2)	0.426(4)	0.77
O (12)	4*e* 0.079(4)	0.416(2)	0.921(5)	0.77
O (H)	4*e* 0.000(5)	0.252(4)	0.196(1)	1.0(2)

Table 4(a) Structural parameters of hydroxyapatite measured at 673 K.

atom	site	x	y	z	B_{eq}/ Å^2
Ca^{2+}(1)	4*f*	0.3333	0.6667	0.0012(6)	1.17
Ca^{2+}(2)	6*h*	0.2471(3)	0.9926(4)	0.2500	0.84
P	6*h*	0.3986(5)	0.3682(4)	0.2500	0.63
O (1)	6*h*	0.3288(7)	0.4847(9)	0.2500	1.26
O (2)	6*h*	0.5850(8)	0.4641(9)	0.2500	1.04
O (3)	12*i*	0.3423(6)	0.2586(7)	0.0687(7)	1.96
O (H)	4*e*	0.0000	0.0000	0.1964(29)	0.89

Table 4(b) The anisotropic thermal parameters ($\times 10^{-4}$) of hydroxyapatite measured at 1473 K.

atom	β_{11}	β_{22}	β_{33}	β_{12}	β_{13}	β_{23}
Ca^{2+}(1)	44(4)	44	40(8)	22	0	0
Ca^{2+}(2)	26(5)	27(5)	49(7)	16(5)	0	0
P	27(7)	16(8)	30(9)	12(6)	0	0
O-(1)	44(20)	36(20)	69(27)	23(18)	0	0
O-(2)	16(20)	53(17)	59(29)	26(16)	0	0
O-(3)	107(13)	55(12)	52(14)	53(10)	-44(11)	-31(11)
O-(H)	29(16)	29	45(89)	14	0	0

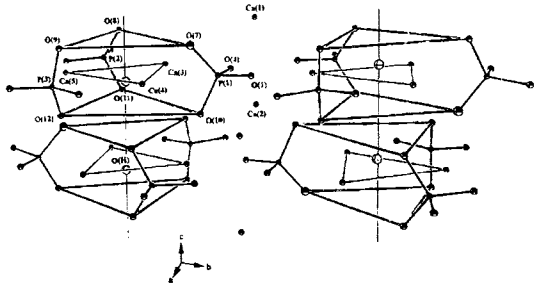

Fig.6 The crystal structure of the monoclinic hydroxyapatite at 300 K with ellipsoids plotted at the 50 % probability level and the arrangements of the calcium and oxygen triangles around the hydroxyl column.

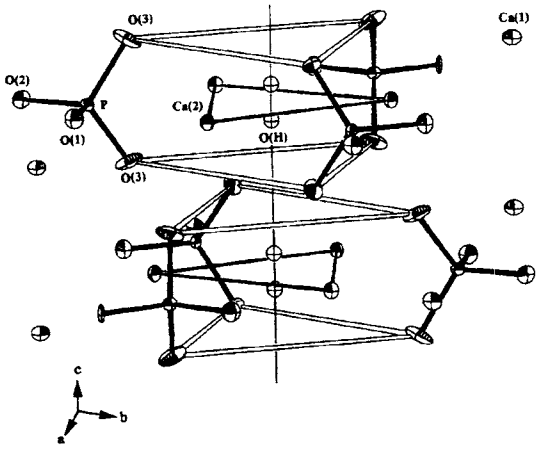

Fig.7 The crystal structure of the hexagonal hydroxyapatite at 673 K with ellipsoids plotted at the 50 % probability level and the arrangements of the calcium and oxygen triangles around the *c*-axis.

hydroxyl column in the hydroxyapatites at 300 K, 473 K and 673 K. The oxygen triangles around a hydroxyl column in the monoclinic hydroxyapatites at 300K and 473 K were appreciably distorted. There are two different sizes of oxygen triangles. The mean O-O distance in one triangle formed by the O(7), O(8) and O(9), which was adjacent to hydroxyl ions, was found to be 5.2 Å and that of another triangle formed by the O(10), O(11) and O(12) was 4.9 Å. The existence of the two different sizes of oxygen triangles seems to be caused by a static force from the hydroxyl ions. In the hexagonal hydroxyapatite at 673 K, the mean O-O distance in the regular oxygen triangle formed by O(3) was found to be 5.06 Å. On the other hand, no differences of the mean Ca-Ca distances in the calcium triangles normal to a hydroxyl column at each temperature were observed. As shown in **Table 6**, the mean P-O distances and O-P-O angles in all structures were calculated to be about 1.55 Å and about 109.5° and no distortion of phosphate tetrahedra were observed. Since the existence of two

Table 5 Interatomic distances ($\times 10^{-1}$ nm) around the hydroxyl columns in hydroxyapatites measured at evaluated temperatures.

Crystal system	monoclinic			hexagonal
Space group	$P2_1/b$	$P2_1/b$		$P6_3/m$
Measured temp. / K	300	473		673
Ca(3)-Ca(4)[1]	4.08(3)	4.06(2)	Ca(2)-Ca(2)[6]	4.113(1)
Ca(3)-Ca(5)[2]	4.14(2)	4.13(3)		
Ca(4)-Ca(5)[1]	4.19(2)	4.19(3)		
mean	4.14	4.13		
O(7)-O(8)[3]	5.11(4)	5.12(4)	O(3)-O(3)[7]	5.066(9)
O(7)-O(9)[2]	5.28(4)	5.31(2)		
O(8)[4]-O(9)	5.15(4)	5.15(3)		
mean	5.18	5.19		
O(10)-O(11)[3]	4.84(4)	4.90(5)		
O(10)-O(12)[2]	4.86(5)	4.92(4)		
O(11)[4]-O(12)	4.86(4)	4.86(6)		
mean	4.85	4.89		
O(O)-O(7)	3.14(6)	3.13(5)	O(H)-O(3)	3.0553(8)
O(O)-O(8)[3]	3.02(6)	2.95(4)		
O(O)-O(9)[2]	3.25(7)	3.37(6)		
mean	3.14	3.15		
O(O)-O(10)	3.30(6)	3.28(6)		
O(O)-O(11)[3]	3.30(5)	3.18(4)		
O(O)-O(12)[2]	3.37(6)	3.26(6)		
mean	3.23	3.24		
O(O)-Ca(3)	2.36(5)	2.39(5)	O(H)-Ca(2)[8]	2.403(4)
O(O)-Ca(4)[1]	2.39(6)	2.35(6)		
O(O)-Ca(5)[2]	2.41(5)	2.44(5)		
mean	2.39	2.39		
O(H)-O(H)[5]	3.445(3)	3.449(3)	O(H)-O(H)[9]	3.455(1)

Symmetry codes:
1) $-x, 1-y, 1-z$; 2) $-x, 1/2-y, -1/2+z$; 3) $x-1, y, z$;
4) $1-x, 1/2-y, 1/2+z$; 5) $-x, 1/2-y, 1/2+z$;
6) $1-y, 1/2-x, z$; 7) $-x+y, -x, z$;
8) $1-y, 1-x+y, 1/2-z$; 9) $-x, -y, 1/2+z$

different size's oxygen triangles and no distortion of the phosphate tetrahedra, the phosphate tetrahedra were definitely rotated. The rotation of phosphate tetrahedra was calculated to be about 6° around the P(1)-O(1), P(2)-O(2) and P(3)-O(3) bond axis against the hydroxyl column. The rotation of phosphate tetrahedra changes the *b*-glide planes in monoclinic hydroxyapatite (low temperature phase) to the mirror planes in hexagonal hydroxyapatite (high temperature phase). Ito *et al.*[21] has reported the rotation of phosphate tetrahedra at about 7° around the P-O(1) bond axis against the *c*-axis in a boron-containing apatite ($Ca_{9.93}(P_{5.84}O_{24})B_{0.83}O_{1.79}$). The boron-containing apatite was synthesized by the flux method and has trigonal symmetry with the space group $P\bar{3}$.

Table 6 Distances (10^{-1} nm) and angles (°) of phosphate tetrahedra in hydroxyapatites at evaluated temperatures.

Crystal system	monoclinic			hexagonal
Space group	$P2_1/b$	$P2_1/b$		$P6_3/m$
Measured temp. / K	300	473		673
P(1)-O(1)	1.57(6)	1.52(3)	P-O(1)	1.543(8)
P(1)-O(4)	1.57(6)	1.53(5)	P-O(2)	1.528(6)
P(1)-O(7)	1.51(4)	1.55(3)	P-O(3)	1.542(4)
P(1)-O(10)	1.51(4)	1.54(4)	P-O(3)[3)]	1.542(4)
mean	1.54	1.54	mean	1.539
P(2)-O(2)1)	1.51(5)	1.55(5)	O(1)-P-O(2)	110.8(4)
P(2)-O(5)	1.57(6)	1.51(3)	O(1)-P-O(3)	110.7(3)
P(2)-O(8)	1.58(3)	1.59(3)	O(2)-P-O(3)	107.9(3)
P(2)-O(11)	1.57(4)	1.56(3)	O(3)-P-O(3)[3)]	108.7(5)
mean	1.56	1.55	mean	109.5
P(3)-O(3)[2)]	1.54(4)	1.55(5)		
P(3)-O(6)	1.52(5)	1.51(4)		
P(3)-O(9)	1.60(3)	1.59(3)		
P(3-O(12)	1.53(4)	1.56(4)		
mean	1.55	1.55		
O(1)-P(1)-O(4)	111(3)	113.0(7)		
O(1)-P(1)-O(7)	111(2)	112.9(4)		
O(1)-P(1)-O(10)	113(2)	112(2)		
O(4)-P(1)-O(7)	107(2)	106 (2)		
O(4)-P(1)-O(10)	105(2)	105.9(4)		
O(7)-P(1)-O(10)	110(3)	106.9(9)		
mean	110	109.5		
O(2)-P(2)[1)]-O(5)[1)]	115(3)	112.7(6)		
O(2)-P(2)[1)]-O(8)[1)]	107(2)	106.0(4)		
O(2)-P(2)[1)]-O(11)[1)]	114(2)	113(2)		
O(5)-P(2)-O(8)	111(2)	108(2)		
O(5)-P(2)-O(11)	106(2)	111(1)		
O(8)-P(2)-O(11)	104(3)	105.9(5)		
mean	110	109.4		
O(3)[2)]-P(3)-O(6)	109(2)	109(1)		
O(3)[2)]-P(3)-O(9)	108(2)	114(2)		
O(3)[2)]-P(3)-O(12)	111(2)	105(1)		
O(6)-P(3)-O(9)	104(2)	105.5(4)		
O(6)-P(3)-O(12)	114(2)	110(2)		
O(9)-P(3)-O(12)	111(2)	113.0(5)		
mean	110	109.4		

Symmetry codes:
1) $-x, 1/2-y, 1/2+z$; 2) $-x, 1-y, 1-z$; 3) $x, y, 1/2-z$

The atomic position of hydrogen in hydroxyl group had been refined using a single crystal hydroxyapatite from Holly Spring by a neutron diffraction measurement.[2] The hydroxyapatite had the hexagonal symmetry, and the atomic parameters of the hydrogen and the oxygen atom in hydroxyl group were determined to be (0, 0, 0.067) and (0, 0, 0.2008), respectively. The hydrogen located on the *c*-axis and hydroxyl ions were aligned in upper and lower direction along a hydroxyl column owing to the repulsion of calcium ions. In the monoclinic hydroxyapatites, the hydroxyl ions showed the ordered arrangement as shown in **Fig.6**; *i.e.* OH, OH, OH, OH in one column and HO, HO, HO, HO in another column and the hydroxyl ions arranged to be anti-paralleled. The monoclinic hydroxyapatite showed the antiferroelectric property from the hydroxyl arrangement.[11] While, the hydroxyl ions in the hexagonal hydroxyapatite existed at the upper and lower direction to

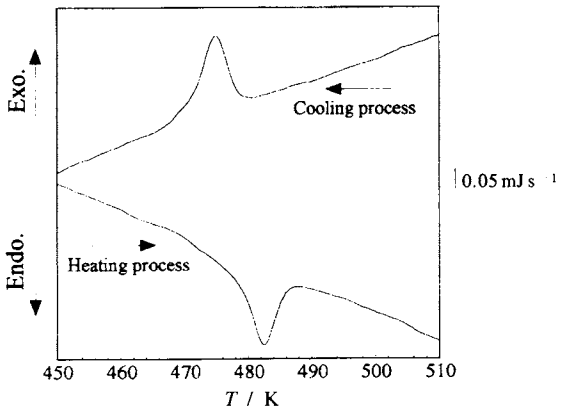

Fig.8 DSC curves for the prepared hydroxyapatite at the rate of 20 K min^{-1}.

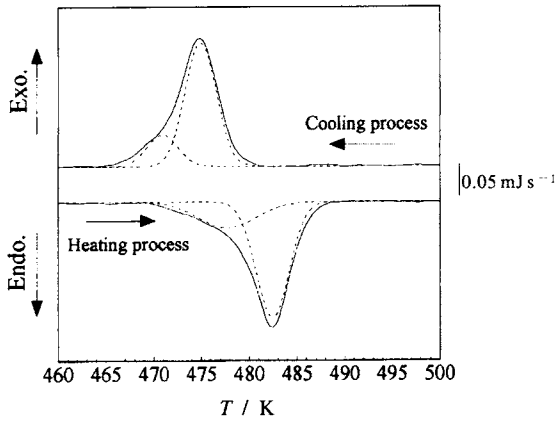

Fig.9 Separated curves of differential scanning calorimetry curves for the prepared hydroxyapatite at the rate of 20 K min $^{-1}$.

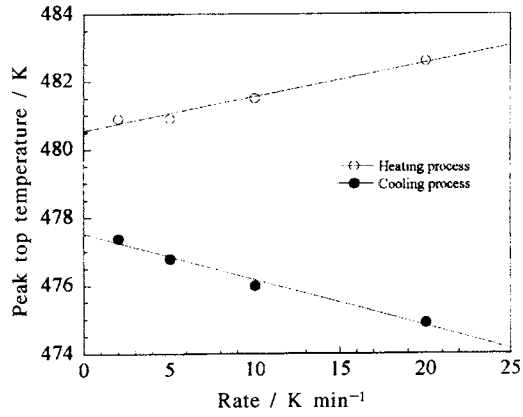

Fig.10 The extrapolated peak temperature lines as a function for the heating rate (a) and cooling rate (b).

the mirror planes at $z = 1/4$, 3/4 as shown in **Fig.7**. The occupancy factor of hydroxyl oxygen was 0.5. Thus, the hexagonal hydroxyapatite had the disordered arrangement of the hydroxyl ions; *i.e.* OH, HO, OH, HO along the c-axis.

4. DSC Study of phase transition

Fig.8 shows the DSC curves in the temperature range of 440 K to 520 K and the endo- and the exothermic peaks are clearly observed at about 480 K. The endo- and exothermic peaks were attributed to the structural changes from the monoclinic to hexagonal symmetry and the phase transition reversibly occurred. The endo- and exothermic peaks showed asymmetric shapes and resolved into two steps. The two step transitions are coincident with the results of structural changes. The phase transition of hydroxyapatite has thought to be the change of hydroxyl arrangement. However, in the present study, the phase transition brought about the rotation of phosphate tetrahedra by 6° against the mirror plane and the order to disorder arrangement of hydroxyls. As shown in **Fig.9**, the endo- and exothermic peaks were deconvoluted by a Gaussian-Lorentian function after removed from the background. The peak at the lower temperature is attributed to the rotation of phosphate tetrahedra and the peak at the higher temperature is attributed to the changes of hydroxyl order to disorder arrangement. The phase transition temperatures were calculated to the peak top temperatures of the observed peaks. **Fig.10** shows the linear extrapolated lines of peak temperatures for the heating and / or cooling rates at 20, 10, 5 and 2 K min $^{-1}$. The extrapolated peak temperatures (a temperature limits to the rate of 0 K mol^{-1}) were calculated to be 480.5(1) K in heating process and 477.5(1) K in cooling process and were almost same value compared with the reported values.[13), 14)] The phase transition enthalpies were calculated from the area of endo- and exothermic peaks measured at the rate of 20 and 10 K min $^{-1}$. The enthalpy values are found to be 127(1) J mol^{-1} on heating, and 130(1) J mol^{-1} on cooling. Suda *et al.*[13)] has reported the enthalpy value of the transition for the hydroxyapatite (Ca/P ratio of 1.68) as 630 J mol^{-1} obtained by DSC measurements. The distinction of the enthalpy values seems to be caused by the difference of the preparation methods, the Ca/P ratio and the hydroxyl contents in its lattice.

Conclusion

The prepared hydroxyapatite with the Ca/P ratio of 1.65 was 98% monoclinic. The following conclusions are obtained. (1) The mean linear thermal expansion coefficients from the temperature range of 300K to 673 K are calculated to be $\alpha_a = 10.8 \times 10^{-6}$ K^{-1} and $\alpha_c = 8.56 \times 10^{-6}$ K^{-1}. (2) In monoclinic hydroxyapatites, two different sizes of oxygen triangles normal to the hydroxyl columns exist and the hydroxyl ions arrange to be ordered. In hexagonal hydroxyapatite, the hydroxyl

ions arrange to be disordered. (3) The phase transition from the monoclinic to hexagonal symmetry occurs reversibly at about 480 K and the phase transition enthalpy is about 130 J mol^{-1}. Further, the two step transitions are observed at the DSC measurements. (4) The phase transition causes the rotation of phosphate tetrahedra at about 6° at lower temperature and the change of hydroxyl order to disorder arrangement at higher temperature.

Acknowledgement

We are grateful to Mr. T. Hirose of Rigaku Co. Ltd. for his permission to use a high temperature X-ray powder diffractometer. We are indebted to the Dr. T. Mitsuhashi of National Institute for Research in Inorganic Materials for using a differential scanning calorimeter.

References

1) A. S. Posner, A. Perloff and A. F. Diorio, *Acta Cryst.* **11**, 308 (1958).
2) M. I. Kay, R. A. Young and A. S. Posner, *Nature* **204**, 1050 (1964).
3) J. C. Elliott, P. E. Mackie and R. A. Young, *Science* **180**, 1055 (1973).
4) E. C. Moreno, T. M. Gregory and W. E. Brown, *J. Res. N. B. S., A. Phys. Chem.*, 773 (1968).
5) E. C. Reynolds, P. E. Riley and E. Story, *Calcif. Tissue Int.* **34**, S52 (1982).
6) S. V. Dorozhkin, *J. Colloid and Inter. Sci.* **191**, 489 (1997).
7) A. S.Posner, *J. Bio. Mater. Res.* **19**, 241-250 (1985).
8) A. Amrah-Bouali, C. Rey, A. Lebugle and D. Bernoche, *Biomaterials* **15**, 269 (1994).
9) D. M. Wieliczka, P. Spencer and R. Z. LeGeros, *J. Dent. Res. 75*, 1865 (1996).
10) K. Sudarsanan, P. E. Mackie and R. A. Young, *Nat. Res. Bull.* **7**, 1331 (1972).
11) J. C. Elliott and R. A. Young, *Nature* **214**, 904 (1967).
12) P. E. Mackie, J. C. Elliott and R. A. Young, *Acta Cryst.* **B24**, 1840 (1972).
13) H. Suda, M. Yashima, M. Kakihana and M. Yoshimura, *J. Phys. Chem.* **99**, 6752 (1995).
14) H. B. Van Rees, M. Mengeot and E. Kastiner, *Mater. Res. Bull.* **8**, 1307 (1973).
15) R. A. Young and D. W. Colcomb, *Calcif. Tissue Int.* **34**, S17 (1982).
16) T. Takahashi, S. Tanase and O. Yamamoto, *Electrochimica Acta* **23**, 363 (1978).
17) K. Yamashita, S. Tanase, T. Umegaki and T. Kanazawa, *J. Mater. Sci. Letter* **9**, 4 (1990).
18) T. Ikoma, A. Yamazaki, S. Nakamura and M. Akao, *J. Solid State Chem.*, (in preparation).
19) F. Izumi, "The Rietveld method," ed. by R. A. Young, Oxford University Press, Oxford, chapter. 13 (1993).
20) J. C. Elliott, "Structure and chemistry of the apatites and other calcium orthophosphates" ed. by J. C. Elliott, Elsevier Press, Amsterdam, chapter. 3 (1994).
21) A. Ito, H. Aoki, M. Akao, N. Miura, R. Otsuka and S. Tsutsumi, *J. Ceram. Soc. Jpn.* **96**, 302 (1988).

要　旨

単斜晶系水酸アパタイトの相変化機構を明らかにすることを目的とし，高温粉末X線回折測定によるRietveld解析及び示差走査熱量測定（DSC）を行った。単斜晶系水酸アパタイトは，湿式法により合成した低結晶性の水酸アパタイトを1473 Kで焼成することにより合成した。Rietveld解析の結果より，合成した水酸アパタイトの単斜晶系率は98％であった。また，低温相では単斜晶系，空間群$P2_1/b$の結晶構造であり，高温相では六方晶系，空間群，$P6_3/m$の結晶構造であることが明らかとなった。単斜晶系水酸アパタイト格子中には2つの異なる大きさの酸素イオンで構成される三角形があり，これはリン酸基がミラー面に対し約6°回転するために生じていた。DSC測定より，単斜晶系から六方晶系への相転移は可逆的であり，昇温過程では480.5(1) K，降温過程では477.5(1) Kに観測できた。また，相変化における活性化エネルギーは，130(1) J mol^{-1}であった。吸熱及び発熱ピークは2段階の過程に分割でき，これは単斜晶系から六方晶系へと相転移する際に，リン酸基の回転と水酸基の秩序－無秩序変化に対応すると考えられる。